MOLECULAR AND CELLULAR BIOLOGY, Jan. 2006, p. 50–62 Vol. 26, No. 1
0270-7306/06/$08.00+0 doi:10.1128/MCB.26.1.50–62.2006
Copyright © 2006, American Society for Microbiology. All Rights Reserved.

Transactivation of Platelet-Derived Growth Factor Receptor α by the GTPase-Deficient Activated Mutant of $G\alpha_{12}$

Rashmi N. Kumar, Ji Hee Ha, Rangasudhagar Radhakrishnan, and Danny N. Dhanasekaran*

Fels Institute for Cancer Research and Molecular Biology, Temple University School of Medicine, Philadelphia, Pennsylvania 19140

Received 12 September 2005/Accepted 12 October 2005

The GTPase-deficient, activated mutant of $G\alpha_{12}$ ($G\alpha_{12}$Q229L, or $G\alpha_{12}$QL) induces neoplastic growth and oncogenic transformation of NIH 3T3 cells. Using microarray analysis, we have previously identified a role for platelet-derived growth factor receptor α (PDGFRα) in $G\alpha_{12}$-mediated cell growth (R. N. Kumar et al., Cell Biochem. Biophys. 41:63–73, 2004). In the present study, we report that $G\alpha_{12}$QL stimulates the functional expression of PDGFRα and demonstrate that the expression of PDGFRα by $G\alpha_{12}$QL is dependent on the small GTPase Rho. Our results indicate that it is cell type independent as the transient expression of $G\alpha_{12}$QL or the activation of $G\alpha_{12}$-coupled receptors stimulates the expression of PDGFRα in NIH 3T3 as well as in human astrocytoma 1321N1 cells. Furthermore, we demonstrate the presence of an autocrine loop involving PDGF-A and PDGFRα in $G\alpha_{12}$QL-transformed cells. Analysis of the functional consequences of the $G\alpha_{12}$-PDGFRα signaling axis indicates that $G\alpha_{12}$ stimulates the phosphatidylinositol 3-kinase (PI3K)-AKT signaling pathway through PDGFR. In addition, we show that $G\alpha_{12}$QL stimulates the phosphorylation of forkhead transcription factor FKHRL1 via AKT in a PDGFRα- and PI3K-dependent manner. Since AKT promotes cell growth by blocking the transcription of antiproliferative genes through the inhibitory phosphorylation of forkhead transcription factors, our results describe for the first time a PDGFRα-dependent signaling pathway involving PI3K-AKT-FKHRL1, regulated by $G\alpha_{12}$QL in promoting cell growth. Consistent with this view, we demonstrate that the expression of a dominant negative mutant of PDGFRα attenuated $G\alpha_{12}$-mediated neoplastic transformation of NIH 3T3 cells.

Heterotrimeric G proteins regulate diverse cellular responses by coupling heptahelical receptors to intracellular effectors (11, 25, 35). Of the different α-subunits that have been analyzed thus far, the α-subunit of the heterotrimeric G protein G12 ($G\alpha_{12}$) shows the most potent mitogenic and oncogenic activities (5, 35). The initial identification of $G\alpha_{12}$ as the transforming oncogene in Ewing's sarcoma cell lines indicated the critical role of $G\alpha_{12}$ in oncogenic signaling (5). Consistent with these observations, serum stimulation or mutational activation of $G\alpha_{12}$ has been shown to stimulate mitogenic pathways in different cell types in addition to inducing neoplastic transformation of Rat-1a and NIH 3T3 fibroblasts (11, 35). NIH 3T3 cells transformed by the GTPase-deficient activated mutant of $G\alpha_{12}$ ($G\alpha_{12}$Q229L, or $G\alpha_{12}$QL) show the characteristic oncogenic phenotype defined by the increased proliferation, anchorage-independent growth, reduced growth factor dependency, attenuation of apoptotic signals, and neoplastic cytoskeletal changes (35). Previously, we have shown that the neoplastic growth of NIH 3T3 cells mediated by the activated mutant $G\alpha_{12}$ involves the expression several unique genes, including platelet-derived growth factor receptor α (PDGFRα) (25). This finding is of critical interest since the signaling pathways involving PDGFR have been strongly correlated with cell proliferation and neoplastic transformation (18), thus pointing to a possible role of PDGFRα in $G\alpha_{12}$QL-mediated oncogenic signaling pathways.

The receptor kinases PDGFRα and PDGFRβ are activated by dimers of PDGF isoforms, PDGF-A, PDGF-B, PDGF-C, and PDGF-D (18). Distinct homo- or heterodimers of PDGFs activate specific homo- or heterodimers of PDGFRα and PDGFRβ in a tissue-specific and context-specific manner (18). The activation of PDGFRs, leading to their dimerization and transphosphorylation at specific tyrosine residues, provides docking sites for different effector molecules such as Shp, phospholipase C-gamma, and phosphatidylinositol 3-kinase (PI3K) (18). Overexpression of PDGFRα or PDGFRβ and the associated autocrine signaling pathways appear to play an etiological role in tumorigenesis and tumorangiogenesis of different neoplasms including basal cell carcinoma (45), gastrointestinal stromal tumors (17), and ovarian cancers (19, 30). It has also been observed that PDGFR, specifically PDGFRβ, is transactivated by G protein-coupled receptors (GPCRs) stimulated by lysophosphatidic acid (LPA) (20), sphingosine-1 phosphate (2), serotonin (33), and angiotensin II (39). However, the underlying signaling mechanisms and the role of the specific G proteins in mediating such transactivation are not fully understood.

In the present study, we demonstrate that $G\alpha_{12}$QL stimulates the expression and transactivation of PDGFRα in NIH 3T3 cells. The ability of transiently expressed $G\alpha_{12}$QL to stimulate the expression of PDGFRα in 1321N1 astrocytoma cells indicates that such a nexus between $G\alpha_{12}$ and PDGFRα is not restricted to one specific cell type. Our results indicate that the expression of PDGFRα stimulated by $G\alpha_{12}$QL involves the small GTPase Rho-dependent signaling pathway. We further determine that the transactivation of PDGFRα by $G\alpha_{12}$QL involves an autocrine signaling loop involving PDGF-A. Transactivation of PDGFRα by $G\alpha_{12}$ leads to the activation of PI3K and AKT-kinase (AKT), with the resultant inhibitory phosphorylation of forkhead transcription factors such as FKHRL1. This, in turn,

* Corresponding author. Mailing address: Fels Institute for Cancer Research and Molecular Biology, Temple University School of Medicine, 3307 N. Broad Street, 556 AHB, Philadelphia, PA 19140. Phone: (215) 707-1941. Fax: (215) 707-5963. E-mail: danny001@temple.edu.

Downloaded from http://mcb.asm.org/ on September 23, 2019 by guest

leads to a decrease in the binding of FKHRL1 to its response elements. We also show that the coexpression of a dominant negative mutant of PDGFRα inhibits neoplastic transformation of NIH 3T3 cells induced by the activated mutant of $G\alpha_{12}$. Taken together with the observation that the inhibition of FKHRL1 leads to an increase in cell proliferation and survival (29), our data presented here identify a novel PDGFR-dependent signaling pathway activated by $G\alpha_{12}$ in promoting neoplastic growth via the PI3K-AKT-FKHRL signaling conduit.

MATERIALS AND METHODS

Cell lines, plasmids, and transfection. Parental NIH 3T3 cells and the previously described pcDNA3-NIH 3T3 and $G\alpha_{12}$Q229L-NIH 3T3 cell lines were maintained as previously described (44). 1321N1 astrocytoma cells were kindly provided by Stephen Cosenza (Fels Institute, Temple University, PA) and were maintained in Dulbecco's modified Eagle's medium (Cellgro, NJ) containing 5% fetal bovine serum. A C terminus-truncated dominant negative mutant of PDGFRα in pLXSN2 vector (22) was a kind gift from Andrius Kazlauskas (Schepens Eye Research Institute, Harvard Medical School, Boston, MA). The cDNA insert encoding truncated PDGFRα was excised from pLXSM2 vector and shuttled into pcDNA3(+) vector at NotI-BamHI sites. Transient expression of $G\alpha_{12}$QL and RhoA-N19 in NIH 3T3 cells was carried out by transfecting the cells (0.7×10^6 cells/60-mm dish) with appropriate expression vectors using Lipofectamine Plus reagent (Invitrogen Technologies, CA). Transient expression using the adenoviral vectors encoding $G\alpha_{12}$QL, RhoA-V14, or RhoA-N19 was carried out by infecting cells (0.5×10^6 cells/60-mm dish) with a multiplicity of infection of viral particles of 600. Transient expression of different constructs in 1321N1 astrocytoma cells was carried out using the Fugene 6 reagent (Roche Diagnostics, IN) according to the manufacturer's protocol. Cells were collected and lysed with modified RIPA buffer (50 mM Tris-HCl [pH 7.4], 1% Nonidet P-40, 0.25% sodium deoxycholate, 150 mM NaCl, 1 mM EGTA, 1 mM sodium fluoride, 1 mM sodium vanadate, 2 μg/ml leupeptin, 4 μg/ml aprotinin, and 1 mM phenylmethylsulfonyl fluoride) at 24 h posttransfection.

Construction of the adenoviral vectors expressing $G\alpha_{12}$QL. A cDNA insert encoding $G\alpha_{12}$QL (1,800 bp) was excised from pcDNA3-$G\alpha_{12}$QL vector (44) using the restriction nucleases KpnI and XbaI. The cohesive ends were blunted and cloned in the EcoRV site of pShuttle-IRES-GFP2 vector (Stratagene, CA) (where IRES is internal ribosome entry site and GFP is green fluorescent protein). The resultant plasmid was linearized using PmeI before it was transformed into *Escherichia coli* BJ5183, in which the homologous recombination event with the plasmid containing adenoviral backbone takes place. The recombinant clones were selected by analysis of the PacI-digested DNA from these clones. The positive recombinant DNA was amplified by transforming it on a suitable *E. coli* strain. The recombinant DNA was cut with PacI and then purified before transfection onto AD293 cells for the virus production. Isolation of virus was carried out by following the standard freeze-thaw protocol. In some instances, further amplification of the virus was carried out by infecting AD293 cells. These recombinant adenoviruses were titrated by plaque assay before target cells were infected. Recombinant adenoviral vectors expressing the constitutively activated RhoA-G14V (RhoA-V14) and the dominant negative RhoA-T19N (RhoA-N19) mutants were kindly provided by Aviv Hassid, University of Tennessee, Memphis, TN (6).

Cell proliferation assay. The CyQUANT Cell proliferation assay kit (Molecular Probes, Inc., Eugene, OR) was used to monitor cell proliferation. Equal numbers of cells (5×10^3 cells/well) were grown in 96-well plates for 24 h and then serum starved for 24 h. The cells were then incubated with the CyQUANT reagent as described by the manufacturer, and fluorescence was monitored using a microplate reader with 485-nm excitation and 535-nm emission filters. A reference standard curve was created as described by the manufacturer for converting the sample fluorescence values into cell numbers.

Semiquantitative RT-PCR. An aliquot of the total RNA (2 μg) was converted into cDNA using a ThermoScript RT-PCR System (Invitrogen Life Technologies, CA). The reverse-transcribed cDNA was subjected to PCR analysis. The following primers were used for the semiquantitative reverse transcription-PCR (RT-PCR): PDGF-A, 5′-GAGATACCCCGGGAGTTGAT and 3′-CTGTCT CCTCCTCCCGATG; PDGF-B specific, 5′-ATCGCCGAGTGCAAGACG and 3′-TCCGAATGGTCACCCGAG; PDGF-C specific, 5′-ACAAGGAACAGA ACGGAGT and 3′-TCAGATACAAATCTTATCCT. The PCR conditions were 2 min of denaturation at 94° followed by cycles of denaturation at 94° for 30 s, annealing at 58° for 1 min, and elongation at 72° for 1 min. To define the optimal number of PCR cycles for linear amplification, PCR products were removed at the end of 20, 24, and 28 cycles. The mouse glyceraldehyde-3-phosphate dehydrogenase (GAPDH)-specific forward (5′-GTGAAGGTCGGTTGTGAACGG-3′) and reverse (5′-GATGCAGGGATGATGTTCTG-3′) primers were used as controls. The amplification products were analyzed by 1% agarose gel electrophoresis.

Immunoprecipitation and immunoblot analysis. Immunoprecipitation of PDGFRα was carried out by incubating cell lysate protein (1 mg each) with 1 μg of PDGFRα antibodies for 16 h at 4°C, followed by incubation with 20 μl of 50% protein A-Sepharose beads (Amersham Biosciences Corp., Piscataway, NJ) for 2 h at 4°C. After repeated washes with cell lysis buffer, the immunoprecipitated proteins were separated by sodium dodecyl sulfate-polyacrylamide gel electrophoresis (SDS-PAGE) and electroblotted onto polyvinylidene difluoride membranes for immunoblot analysis. Immunoblot analyses of lysate or immunoprecipitated proteins were carried out according to previously published procedures (5). Antibodies to $G\alpha_{12}$ (sc-409), PDGFRα (sc-338), PDGFRβ (sc-432), PDGF-A (sc-7958), ROCK-1 (sc-6056), and AKT (sc-1618) were purchased from Santa Cruz Biotechnology, Inc., CA. Antibodies to phospho-FKHRL1-Thr32 (no. 06-952), FKHRL1 (no. 6-951) and phosphotyrosine (clone 4G10, no. 05-321) were purchased from Upstate Signaling Solutions (Charlottesville, VA). Antibodies to GAPDH (no. 4300) and p-AKT Ser473 (no. 9271) were purchased from Ambion, Inc. (Austin, TX) and Cell Signaling Technology, Inc. (Beverly, MA), respectively. Peroxidase-conjugated anti-mouse immunoglobulin G and rabbit immunoglobulin G were purchased from Amersham Biosciences UK, Ltd. (Buckinghamshire, England) and Promega (Madison, WI), respectively.

Rho activation assay. Bacterial expression vector pGEX-2T encoding a glutathione S transferase (GST)-fused Rho-binding domain (GST-RBD) of rhotekin (amino acids 8 to 89) was kindly provided by Gary Bokoch, Scripps Research Institute, La Jolla, CA. GTP-bound Rho was precipitated using GST-RBD according to previously published methods (3, 36, 38). Briefly, cells were lysed in Rho-binding buffer (25 mM HEPES, pH 7.5, 150 mM NaCl, 1% Igepal CA-630, 10 mM $MgCl_2$, 1 mM EDTA, 10% glycerol, and protease inhibitor cocktail), and the clarified cell lysates were incubated with GST-RBD-bound glutathione-Sepharose 4B beads (30 μl of 50% slurry) at 4°C for 20 min. The beads were washed four times with ice-cold Rho-binding buffer and resuspended in Laemmli's sample buffer. The pulled-down Rho-GTP was identified by immunoblot analysis using Rho-A antibodies.

PDGFRα immunocomplex kinase assay. An immunocomplex kinase assay to monitor the kinase activity of PDGFRα was carried out using previously published methods with appropriate modifications (46). To monitor the autophosphorylating kinase activity of PDGFRα, PDGFRα was immunoprecipitated from cell lysates using antibodies to PDGFRα (as described above). After repeated washes, the immunoprecipitates were resuspended in 50 μl of kinase buffer (25 mM HEPES, pH 7.4, 5 mM $MgCl_2$ and 0.2 mM EDTA) and subjected to an auto-kinase assay by incubating them with 20 μM [γ-^{32}P]ATP (5,000 cpm/pmol) for 30 min at 30°C. The phosphorylated proteins were separated by SDS-PAGE, followed by autoradiography.

p160ROCK immunocomplex assay. p160ROCK was immunoprecipitated from 50 μg of cell lysates using antibodies to p160ROCK (sc-6056). The immunoprecipitates were washed twice with the lysis buffer (25 mM HEPES pH 7.6, 0.1% Triton X-100, 300 mM NaCl, 20 mM β-glycerophosphate, 1.5 mM $MgCl_2$, 0.2 mM EDTA, 2 μM dithiothreitol [DTT], 1 mM sodium vanadate, 2 μg/ml leupeptin, 4 μg/ml aprotinin) followed by two washes with reaction buffer (20 mM HEPES, pH 7.6, 20 mM β-glycerophosphate, 1 mM $MgCl_2$, and 1 mM sodium vanadate). The kinase reaction was carried out by resuspending the immunoprecipitates in 40 μl of reaction buffer containing 20 μM [γ-^{32}P]ATP (5,000 cpm/pmol) and 5 μg of myelin basic protein (Sigma-Aldrich, St. Louis, MO) as a substrate according to previously published procedures (26). The reaction mixture was incubated for 30 min at 30°C. The phosphorylated myelin basic protein bands were visualized by SDS-PAGE, followed by autoradiography. The radioactive myelin basic protein bands were excised and quantified in a liquid scintillation counter.

Immunocomplex AKT assay. AKT was immunoprecipitated from 500 μg of cell lysates using antibodies to AKT (sc-1618). The immunoprecipitates were washed twice with the lysis buffer (25 mM HEPES, pH 7.6, 0.1% Triton X-100, 300 mM NaCl, 20 mM β-glycerophosphate, 1.5 mM $MgCl_2$, 0.2 mM EDTA, 2 μM DTT, 1 mM sodium vanadate, 2 μg/ml leupeptin, 4 μg/ml aprotinin), followed by two washes with reaction buffer (20 mM HEPES, pH 7.6, 20 mM β-glycerophosphate, 1 mM $MgCl_2$, and 1 mM sodium vanadate). The kinase reaction was carried out by resuspending the immunoprecipitates in 40 μl of reaction buffer containing 20 μM [γ-^{32}P]ATP (5,000 cpm/pmol) and 2 μg of purified recombinant FKHR protein (14-343; Upstate, NY) as a substrate. The reaction was incubated for 30 min at 30°C. The phosphorylated FKHR bands

Downloaded from http://mcb.asm.org/ on September 23, 2019 by guest

were visualized by SDS-PAGE, followed by autoradiography. The radioactive FKHR bands were excised and quantified in a liquid scintillation counter.

PI3K assay. PI3K assays were carried out according to published procedures (34). Cell lysates were prepared by lysing the cells in PI3K lysis buffer (25 mM HEPES, pH 7.4, 150 mM NaCl, $MgCl_2$, 5 mM, 0.2 mM EDTA, 0.1% Triton X-100, 0.5 mM DTT, 0.1 mM phenylmethylsulfonyl fluoride, 2 μg/ml leupeptin, 4 μg/ml aprotinin) for 20 min at 4°C and removing the cell debris by centrifuging at 18,000 × *g* for 10 min. PDGFRα was immunoprecipitated from 200 μg of lysate protein (as described above). The immunoprecipitates were sequentially washed with PI3K lysis buffer, followed by three washes with PI3K lysis buffer lacking Triton X-100. The PI3K reaction was carried out by resuspending the PDGFRα immunocomplex in 35 μl of PI3K reaction buffer (25 mM HEPES, pH 7.4, 5 mM $MgCl_2$, and 0.2 mM EDTA) and incubating with 50 μM ATP, 5 μCi of [γ-^{32}P]ATP, and 5 μg of phosphotidylinositol plus 5 μg of phosphoserine for 5 min at 25°C. The reaction was stopped by the addition of 300 μl of CH_3OH · 1 N HCl (1:1). The phosphorylated inositols were separated on a 1% potassium oxalate-coated thin-layer chromatography (TLC) plate using $CHCl_3$ · CH_3OH · 4 M NH_4OH (9:7:2) as the developing solvent (34).

Electrophoretic mobility shift assay. Nuclear extracts from pcDNA3-and $G\alpha_{12}$QL-NIH 3T3 cells were prepared according to previously published procedures (29). The oligonucleotides used were the following: forward, 5′-TTAAATAAATAAGTAAATAAATAAAC-3′; reverse, 5′-GTTTATTTATTTACTTATTTATTTAA-3′. The annealed double-stranded oligonucleotides (25 pmol) were end labeled with 20 μM [γ-^{32}P]ATP (5,000 cpm/pmol) and purified by G-25 spin columns (Amersham Pharmacia, MA). A total of 5 μg of nuclear extracts was mixed with 1 μg of salmon sperm DNA (Gibco BRL, CA) and radiolabeled probes (50,000 cpm) with or without unlabeled competitor probes. For supershift assays, nuclear extracts were preincubated with 10 μg of FKHRL1-antibodies (06-951) from Upstate Signaling Solutions, (Charlottesville, VA) for 30 min at 25°C prior to the labeled probes. DNA-protein complexes were resolved on a 5% nondenaturing PAGE gel in 0.25× TBE buffer (50 mM Tris, 50 mM boric acid, and 1 mM EDTA). The gels were dried and autoradiographed.

Focus formation assay. An NIH 3T3 cell focus formation assay was carried out as previously described (43). Parental NIH 3T3 cells were transfected with pcDNA3 vectors encoding $G\alpha_{12}$QL (5 μg) with or without dominant negative PDGFRα (DN-PDGFRα; 5 μg) using the calcium phosphate transfection method. The control group included transfections with empty pcDNA3 vector (10 μg). Transfected NIH 3T3 cells were cultured in the presence of 5% serum, and transformed foci were stained and scored after 14 days.

RESULTS

Activated mutant of $G\alpha_{12}$ stimulates cell proliferation and PDGFRα expression. Expression of constitutively activated mutants of $G\alpha_{12}$ stimulates proliferation in many cell types including NIH 3T3 cells (35). NIH 3T3 cells overexpressing $G\alpha_{12}$QL ($G\alpha_{12}$QL-NIH 3T3) show increased proliferation even under reduced serum growth conditions (Fig. 1A). Since our previous transcriptional profiling data of $G\alpha_{12}$QL-NIH 3T3 cells has indicated a role for PDGFRα in $G\alpha_{12}$QL-mediated oncogenic growth of NIH 3T3 cells (25), we analyzed the expression of PDGFRα in $G\alpha_{12}$QL-NIH 3T3 cells. Results from such analyses indicated that the protein levels of PDGFRα are increased by fourfold in $G\alpha_{12}$QL-NIH 3T3 cells compared to the pcDNA3-NIH 3T3 vector control cells (Fig. 1B). Next, we examined the possibility that the observed increased expression of PDGFRα was due to the presence of $G\alpha_{12}$QL and not to the nonspecific phenotype of the transformed or highly proliferating cells. NIH 3T3 cells transformed by activated $G\alpha_{13}$ ($G\alpha_{13}$QL) can be used to assess this possibility, since the activated mutant of $G\alpha_{13}$, which shares 67% amino acid identity with $G\alpha_{12}$, has been shown to transform NIH 3T3 cells readily through signaling pathways distinctly different from those of $G\alpha_{12}$ (36). With this view, we analyzed the expression of PDGFRα in NIH 3T3 cells transformed by the activated mutant of $G\alpha_{13}$. Results from such analysis indicated that the increased expression of PDGFRα is observed only in cells transformed by $G\alpha_{12}$QL (Fig. 1C). Thus, our results demonstrate that the increased expression of PDGFRα is not a generic function of a transformed or highly proliferating cellular phenotype but, rather, is due to specific pathways activated by $G\alpha_{12}$QL.

We next investigated whether PDGFRα can be stimulated by activation of a specific GPCR that interacts with $G\alpha_{12}$. Studies from our laboratory have shown that the bioactive phospholipid LPA stimulates the wild-type (WT) $G\alpha_{12}$ in NIH 3T3 cells (37). Therefore, NIH 3T3 cells stably expressing $G\alpha_{12}$WT ($G\alpha_{12}$WT-NIH 3T3) were serum starved for 24 h and stimulated with 20 μM LPA for 6 h. Similarly treated $G\alpha_{12}$QL-NIH 3T3 cells and pcDNA3-NIH 3T3 cells were used as controls. The cell lysates were subjected to SDS-PAGE followed by immunoblot analysis using anti-PDGFRα. The same blot was probed with GAPDH antibodies to monitor equal protein loading. The results indicate that the activation of $G\alpha_{12}$WT by stimulation with LPA leads to an increase in PDGFRα levels (Fig. 1D), comparable to that of mutationally activated $G\alpha_{12}$. Thus, our results demonstrate that the receptor-mediated activation as well as the mutational activation of $G\alpha_{12}$ leads to an increase in the expression of PDGFRα.

$G\alpha_{12}$QL stimulates the expression of PDGFRα through Rho. We next investigated the signaling mechanism that couples $G\alpha_{12}$ to PDGFRα expression and associated transactivation. Studies from our laboratory as well as others have shown that $G\alpha_{12}$ regulates diverse sets of signaling pathways primarily through the activation of the Rho family of GTPases (11). It has been observed that $G\alpha_{12}$QL stimulates the expression of many different growth-promoting genes through the signaling pathways regulated by the small GTPase Rho (14). In this context, it is interesting that PDGFRα promoter contains several Rho-responsive elements such as NF-κB, GATA, CCAAT, and AP-1 sites (24). Therefore, we examined whether the upregulation and subsequent transactivation of PDGFRα by $G\alpha_{12}$QL involved a Rho-dependent signaling pathway. $G\alpha_{12}$QL-NIH 3T3 cells were treated with 10 μM Y27632, an inhibitor of the Rho effector kinase p160ROCK for 16 h (conditions which effectively block the p160ROCK enzymatic activity [23]), and the expression as well as the phosphorylation levels PDGFRα was monitored. The ability of Y27632 to inhibit p160ROCK in these lysates was also monitored using an in vitro p160ROCK assay. Results indicated that Y26732 treatment completely inhibited a $G\alpha_{12}$QL-mediated increase in PDGFRα levels (Fig. 2A), thus pointing to a role for the Rho-p160ROCK signaling pathway in the transactivation of PDGFRα by $G\alpha_{12}$QL.

Based on the results presented here, it can be inferred that Rho is downstream of $G\alpha_{12}$ in mediating the increased expression of PDGFRα. To further establish that the expression of PDGFRα stimulated by $G\alpha_{12}$QL involves Rho, we investigated whether the coexpression of a dominant negative inhibitory mutant of RhoA (RhoA-N19) inhibits $G\alpha_{12}$QL-mediated increased expression of PDGFRα and, if so, whether the expression of an activated mutant of Rho (RhoA-V12) increases the expression of PDGFRα similar to that of $G\alpha_{12}$. We carried out such an analysis by transiently expressing the activated mutant of RhoA-V12 in NIH 3T3 cells using adenoviral vectors. NIH 3T3 cells were infected with adenoviral vectors encoding $G\alpha_{12}$QL, RhoA-N19, $G\alpha_{12}$QL+RhoA-N19, RhoA-V12, or empty vector for 24 h, and the expression of PDGFRα was

Downloaded from http://mcb.asm.org/ on September 23, 2019 by guest

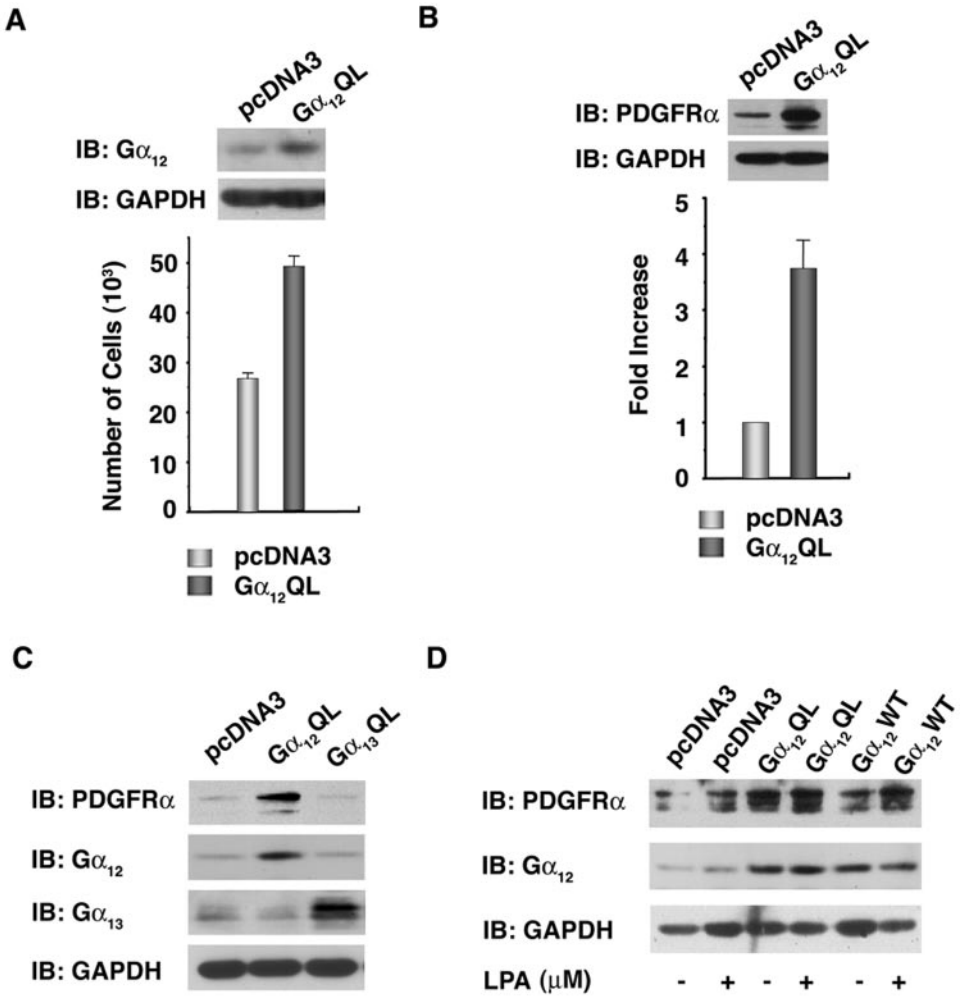

FIG. 1. Activation of $G\alpha_{12}$ stimulates the expression of PDGFRα in NIH 3T3 cells. (A) $G\alpha_{12}$QL mediates serum-independent growth of NIH 3T3 cells. Vector control and $G\alpha_{12}$QL-transformed NIH 3T3 cells (4×10^5) were plated on 100-mm plates. Lysates (100 μg) from these cells were subjected to immunoblot analysis with antibodies to $G\alpha_{12}$ for the overexpression of $G\alpha_{12}$QL and also stripped and reprobed with GAPDH to monitor equal loading (top). Proliferation of these cells in serum-free medium was monitored as described under in Materials and Methods (bottom). (B) $G\alpha_{12}$QL mediates increase in PDGFRα expression. Lysates from 24-h serum-starved pcDNA3- and $G\alpha_{12}$QL-NIH 3T3 cells were subjected to immunoblot analysis using antibodies to PDGFRα (top). The expression levels were quantified using Kodak 1D image analysis software. Results are presented as the increase in expression (*n*-fold) over the vector control cells (mean ± SEM; $n = 10$). (C) Activated $G\alpha_{12}$, not $G\alpha_{13}$, stimulates the expression of PDGFRα. pcDNA3-NIH 3T3 cells, $G\alpha_{12}$QL-NIH 3T3 cells, and $G\alpha_{13}$QL-NIH 3T3 were plated (1×10^6 cells per 100-mm culture dish) and allowed to grow for 24 h, after which the cells were serum starved for 24 h. Lysates were prepared and subjected to SDS-PAGE. Immunoblot analyses were carried out using anti-PDGFRα. Immunoblot analysis was carried out with antibodies to $G\alpha_{12}$ or $G\alpha_{13}$ to monitor the expression of the respective α-subunits. The blot was stripped and reprobed with GAPDH to monitor equal protein loading. Results are from a representative experiment ($n = 3$). (D) PDGFRα levels increase upon stimulation of WT $G\alpha_{12}$ ($G\alpha_{12}$WT) with LPA. pcDNA3-NIH 3T3 cells, $G\alpha_{12}$QL-NIH 3T3 cells, and $G\alpha_{12}$WT-NIH 3T3 cells and were plated (1×10^6 cells per 100-mm culture dish) and allowed to grow for 24 h. The cells were then serum starved for 24 h and stimulated with 20 μM LPA. After 6 h, the lysates were prepared and subjected to SDS-PAGE. Immunoblot analyses were carried out using anti-PDGFRα. The blot was stripped and reprobed with antibodies to $G\alpha_{12}$ and GAPDH to monitor $G\alpha_{12}$ expression and equal protein loading, respectively. Results from a typical ($n = 3$) experiment are presented. IB, immunoblot.

monitored using immunoblot analysis. The inhibitory role of RhoA-N19 and the stimulatory role of RhoA-V12 were monitored by the activated Rho-GTP binding assay using GST-RBD (3, 36, 38). Results indicated that the coexpression of RhoA-N19 blunted the ability of $G\alpha_{12}$QL to stimulate the expression of PDGFRα (Fig. 2B, lane 2 versus lane 4), further validating the involvement of Rho in $G\alpha_{12}$-mediated expression of PDGFRα. It should be noted here that the dominant negative mutants of other small GTPases such as Ras-N17, Rac-N17, and CDC42-N17 failed to produce such attenuation of $G\alpha_{12}$QL-mediated enhanced expression of PDGFRα (data not shown). If Rho is involved in $G\alpha_{12}$QL-mediated expression of PDGFRα, the expression of a constitutively activated mutant of Rho should enhance the expression of PDGFRα similar to that of $G\alpha_{12}$QL. In accordance with this assumption, the transient expression of the activated mutant of RhoA in these cells stimulated the expression of PDGFRα similar to that of $G\alpha_{12}$QL (Fig. 2B, lane 2 versus lane 5). Together, these findings establish that $G\alpha_{12}$QL stimulates the expression of PDGFRα via a Rho-mediated signaling pathway.

Downloaded from http://mcb.asm.org/ on September 23, 2019 by guest

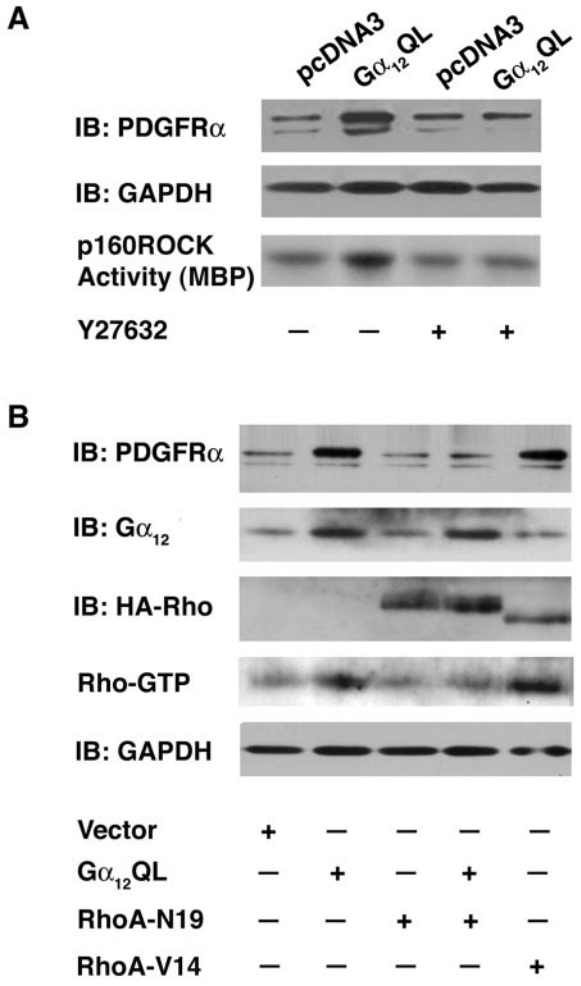

FIG. 2. $G\alpha_{12}$QL stimulation of PDGFRα-expression involves Rho-dependent signaling pathway. (A) $G\alpha_{12}$QL stimulates the expression of PDGFRα through Rho kinase p160ROCK. $G\alpha_{12}$QL-NIH 3T3 and pcDNA3-NIH 3T3 cells were serum starved for 24 h. Prior to lysis, the cells were treated with the p160ROCK inhibitor, Y27632 (20 μM), for 16 h along with nontreated controls. The lysates (50 μg) were subjected to immunoblot analysis with anti-PDGFRα antibodies. The blot was also reprobed with anti-GAPDH to monitor equal loading of proteins. The ability of Y26732 to inhibit p160ROCK was monitored using a p160ROCK immunocomplex kinase assay as described in Materials and Methods using myelin basic protein (MBP) as a substrate. The phosphorylated myelin basic protein was separated by 12% SDS-PAGE and visualized by autoradiography. (B) $G\alpha_{12}$QL requires functional Rho for the expression of PDGFRα. NIH 3T3 cells were infected with the adenoviral expression vectors encoding $G\alpha_{12}$QL, Gα12QL plus three-HA-tagged N19-RhoA (where HA is hemagglutinin) or HA-tagged V12-RhoA (multiplicity of infection of 600). After 24 h, the lysates from these cells (100 μg) were subjected to immunoblot analysis with antibodies to PDGFRα. The blot was further probed with antibodies to $G\alpha_{12}$ and HA epitope to monitor the expression of the exogenous cDNAs. Please note that the difference in the mobility of RhoA-N19 is due to the three-HA epitope. Rho-inhibition by RhoA-N19 and the constitutively activated status of RhoA-V14 mutants were monitored by a Rho activation assay using a GST-RBD binding assay as described in Materials and Methods. The blot was reprobed with GAPDH antibodies to monitor equal loading of proteins. IB, immunoblot.

Activated mutant of $G\alpha_{12}$ stimulates the activity of PDGFRα. Activation of PDGFRα involves ligand-dependent dimerization of the receptor tyrosine kinase followed by the transphosphorylation of specific tyrosine residues (18). Therefore, we sought to investigate whether the $G\alpha_{12}$QL-upregulated PDGFRα undergoes such activation. Analyses of the expression levels and the tyrosine phosphorylation profiles of PDGFRα in $G\alpha_{12}$QL-NIH 3T3 cells indicated that $G\alpha_{12}$QL stimulated the expression as well as phosphorylation of PDGFRα in these cells (Fig. 3A). The phosphorylation levels of PDGFRα in relation to its expression levels were increased by 60% ± 9% (mean ± standard error of the mean [SEM]; $n = 6$) over control values ($P = 0.01$). Since previous studies have shown that such an increase in the phosphorylation levels of PDGFR can elicit mitogenic responses in different cell types (32, 42), our results identify PDGFRα as a novel player in $G\alpha_{12}$-mediated mitogenic signaling. In this context, it is of interest to analyze whether $G\alpha_{12}$ also stimulates the expression and activation of closely related PDGFRβ. Lysates from cells expressing $G\alpha_{12}$QL were subjected to parallel immunoblot analysis with antibodies to PDGFRα and PDGFRβ. Results from these studies showed that $G\alpha_{12}$QL had no effect on PDGFRα expression or activity (Fig. 3B), thus clearly establishing the ability of $G\alpha_{12}$ to specifically stimulate and transactivate PDGFRα (Fig. 3A) and not PDGFRβ (Fig. 3B).

To further demonstrate that the expression and activation of PDGFRα are directly in response to the expression of the activated $G\alpha_{12}$, we transiently expressed $G\alpha_{12}$QL in NIH 3T3 cells and monitored the expression of PDGFRα. An expression vector containing a cDNA insert encoding $G\alpha_{12}$QL was transfected into the parental NIH 3T3 cells. The cells were lysed at 48 h posttransfection, and the lysates were examined for the increased expression and phosphorylation by immunoblot analysis using antibodies to PDGFRα and phosphotyrosine (P-Tyr) antibodies, respectively. The immunoblot analysis clearly indicated that $G\alpha_{12}$QL stimulated the expression of PDGFRα even when it was expressed transiently (Fig. 3C). Reprobing with antibodies to P-Tyr indicated that the tyrosine phosphorylation of PDGFRα is also increased in these cells in response to $G\alpha_{12}$QL (Fig. 3C).

Next, we investigated whether the observed expression of PDGFRα stimulated by the activated mutant of $G\alpha_{12}$ is cell type dependent. Since it has been shown that $G\alpha_{12}$ plays a dominant role in the proliferation of astrocytoma cells (1, 7) and PDGFRs play a critical role in the growth of astrocytomas (12, 27), we analyzed the role of $G\alpha_{12}$ in the expression of PDGFRα in astrocytoma cell line 1321N1. An activated mutant of $G\alpha_{12}$ was transiently expressed in astrocytoma cells using pcDNA3 vectors encoding $G\alpha_{12}$QL for 24 h, and the expression of PDGFRα was monitored using immunoblot analysis. Results indicated that the transient expression of $G\alpha_{12}$QL in these cells stimulated the expression of PDGFRα (Fig. 3D), further validating the ability of $G\alpha_{12}$QL to stimulate the expression of PDGFRα in two distinctly different cell types.

Previous studies have shown that thrombin stimulates a mitogenic response in 1321N1 astrocytoma cells by coupling to $G\alpha_{12}$ (1). Microinjection of antibodies to $G\alpha_{12}$ blocked the thrombin-stimulated mitogenic response in 1321N1 astrocytoma cells, thus indicating that $G\alpha_{12}$ is critically required for thrombin-mediated proliferation of these cells (1). It has also

Downloaded from http://mcb.asm.org/ on September 23, 2019 by guest

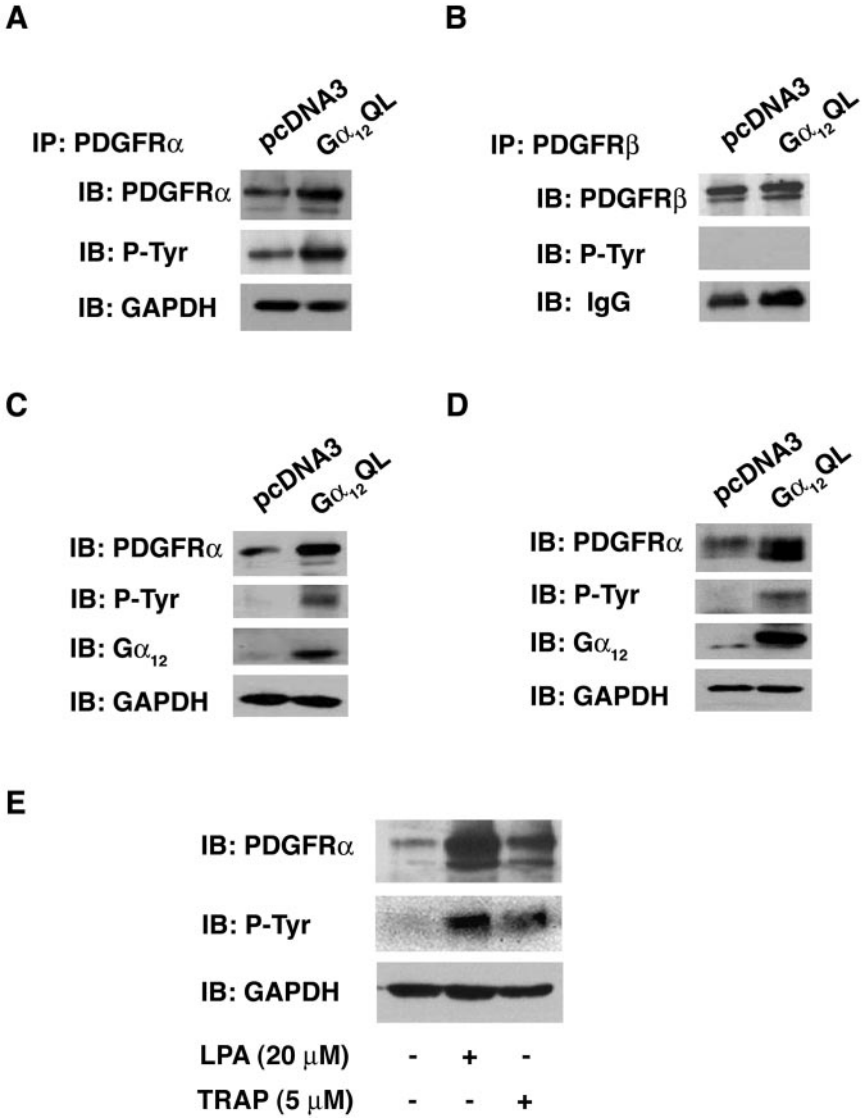

FIG. 3. $G\alpha_{12}$ and GPCRs that activate $G\alpha_{12}$ stimulate the expression and transactivation of PDGFRα. (A) $G\alpha_{12}$QL stimulates the expression and activation of PDGFRα. Lysates (500 μg) from $G\alpha_{12}$QL-NIH 3T3 cells along with vector control were immunoprecipitated with antibodies to PDGFRα and subjected to immunoblot analysis with antibodies to P-Tyr. After stripping, the blot was sequentially reprobed with PDGFRα and GAPDH. (B) $G\alpha_{12}$QL does not stimulate the expression of PDGFRβ. Lysates (500 μg) from $G\alpha_{12}$QL-NIH 3T3 cells along with vector control were subjected to immunoprecipitation with antibodies to PDGFRβ, followed by immunoblot analysis with antibodies to P-Tyr. The blot was stripped and reprobed with PDGFRβ and GAPDH. (C) Transient expression of $G\alpha_{12}$QL stimulates the expression and transactivation of PDGFRα in NIH 3T3 cells. NIH 3T3 cells were transfected with the expression vector pcDNA3 or pcDNA3 encoding $G\alpha_{12}$QL (8 μg) using Lipofectamine Plus reagent. After 24 h, the lysates (100 μg) from the transfectants were subjected to immunoprecipitation using antibodies to PDGFRα, following which an immunoblot analysis was carried out with antibodies to P-Tyr. The blot was stripped and reprobed with antibodies to PDGFRα. The blot was further probed with antibodies to $G\alpha_{12}$ and GAPDH to monitor $G\alpha_{12}$QL-expression and equal loading, respectively. (D) Transient expression of $G\alpha_{12}$QL stimulates the expression and transactivation of PDGFRα in 1321N1 astrocytoma cells. 1321N1 astrocytoma cells were transfected with vectors encoding $G\alpha_{12}$QL or pcDNA3 vector (5 μg) using Fugene 6 reagent. After 24 h, the lysates (100 μg) from the transfectants were subjected to immunoprecipitation using antibodies to PDGFRα, following which an immunoblot analysis was carried out with antibodies to P-Tyr. The blot was stripped and reprobed with antibodies to PDGFRα. The blot was stripped and reprobed with antibodies to $G\alpha_{12}$ and GAPDH to monitor $G\alpha_{12}$QL-expression and equal loading, respectively. (E) GPCR ligands, LPA and TRAP, stimulate the expression and transactivation of PDGFRα in 1321N1 astrocytoma cells. 1321N1 astrocytoma cells were serum starved for 24 h. After starvation, the cells were stimulated with 20 μM LPA or 5 μM TRAP for 6 h. The cell lysates (100 μg) were subjected to immunoblot analysis with antibodies to P-Tyr. The blot was further reprobed with antibodies to GAPDH to monitor equal loading of proteins. IP, immunoprecipitate; IB, immunoblot.

been shown that LPA can stimulate the proliferation of these cells by coupling to $G\alpha_{12}$ (40). Therefore, we investigated whether LPA or thrombin stimulates the expression of PDGFRα in these cells. 1321N1 astrocytoma cells were serum starved for 24 h, following which they were stimulated with 20 μM LPA or 5 μM thrombin receptor-activating peptide (TRAP) for 6 h. Lysates from these cells were subjected to immunoblot analysis using antibodies to PDGFRα and P-Tyr. Results from such

Downloaded from http://mcb.asm.org/ on September 23, 2019 by guest

analysis indicated that activation of LPA as well as thrombin receptors by their cognate ligands stimulated the expression and tyrosine phosphorylation of PDGFRα in 1321N astrocytoma cells (Fig. 3E). Together with the observation that LPA stimulates the expression of PDGFRα in cells expressing WT $G\alpha_{12}$, (Fig. 1D), these results demonstrate that GPCRs that link to $G\alpha_{12}$ stimulate the expression and activation of PDGFRα in two distinctly different cell types.

$G\alpha_{12}$QL-mediated neoplastic growth involves the PDGF-PDGFRα autocrine loop. It has been observed that neoplastic transformation often involves the formation of autocrine signaling pathways through which the transformed cells become less dependent on exogenous growth factors (16). Such oncogene-specific autocrine loops involving different receptor tyrosine kinases including PDGFR have been well characterized (9, 41). To determine whether any of the known PDGFRα ligands are involved in such an autocrine signaling loop stimulated by the activated mutant of $G\alpha_{12}$, we investigated the expression of the known PDGFRα ligands, namely, PDGF-A, PDGF-B, and PDGF-C in $G\alpha_{12}$QL-expressing NIH 3T3 cells. Using RNAs isolated from $G\alpha_{12}$QL-NIH 3T3 cells along with the pcDNA3-vector controls, semiquantitative RT-PCR analyses were carried out to monitor the expression of the PDGF-A, PDGF-B, or PDGF-C. These results indicate that the expression of PDGF-A is increased in $G\alpha_{12}$QL cells by twofold in comparison with the vector control cells (Fig. 4A). In addition, a relatively modest increase in the expression of PDGF-C can also be seen with little or no change in the expression of PDGF-B.

To further validate that $G\alpha_{12}$QL stimulates the expression of PDGF-A that can play a role in the activation of PDGFRα, we analyzed the expression of PDGF-A in the lysates from $G\alpha_{12}$QL-NIH 3T3 cells by immunoblot analysis using antibodies to PDGF-A. Results indicated the increased expression of PDGF-A in $G\alpha_{12}$QL-NIH 3T3 cells compared to the vector control cells (Fig. 4B). To establish this further, we carried out a bioassay for PDGFRα-activation in which we analyzed (i) whether the conditioned medium (CM) from $G\alpha_{12}$QL-NIH 3T3 cells stimulates PDGFRα phosphorylation in vector control cells and, if so, (ii) whether the immunodepletion of PDGF-A in this medium abrogates such an effect on PDGFRα phosphorylation. To answer these questions, the medium in which $G\alpha_{12}$QL-NIH 3T3 cells were grown in the absence of serum for 24 h ($G\alpha_{12}$QL-CM) was collected and added to 24-h serum-starved vector control pcDNA3-NIH 3T3 cells. Following 10 min of incubation with the CM, the lysates from these cells along with experimental control groups were subjected to immunoblot analyses with antibodies to PDGFRα, followed by stripping and reprobing with anti-P-Tyr antibodies. Results indicated that the vector control cells incubated with the CM showed an increase in the phosphorylation levels of PDGFRα (Fig. 4C). When the phosphorylation levels of PDGFRα in vector control cells in response to $G\alpha_{12}$QL-CM were monitored, the results indicated that there was a twofold increase (normalized to the expression levels; $n = 3$) in the phosphorylation levels of PDGFRα. However, when PDGF-A in this culture medium was depleted by immunoprecipitation with antibodies to PDGF-A prior to stimulating PDGFRα, the phosphorylation of PDGFRα was drastically reduced (<75%) (Fig. 4C). Taken together (Fig. 4A to C), these findings

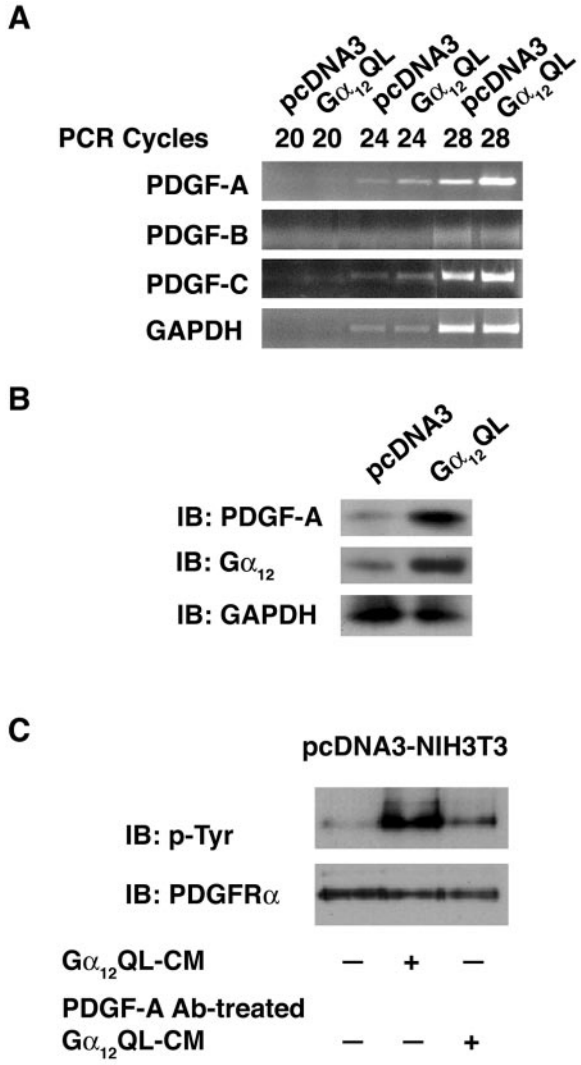

FIG. 4. $G\alpha_{12}$QL stimulates a PDGF-PDGFRα-mediated autocrine loop. (A) Expression of PDGF-A and PDGF-C in $G\alpha_{12}$QL-NIH 3T3 cells. Semiquantitative RT-PCR was carried out using total RNA in $G\alpha_{12}$QL-NIH 3T3 and pcDNA3-NIH 3T3 cells with primers specific to PDGF-A, PDGF-B, and PDGF-C using conditions described in Material and Methods. RT-PCR using GAPDH-specific primers was used as loading control. (B) Expression of PDGF-A in $G\alpha_{12}$QL-NIH 3T3 cells. Lysates from 24-h serum-starved pcDNA3- and $G\alpha_{12}$QL-NIH 3T3 cells were subjected to immunoblot analysis using antibodies to PDGF-A and $G\alpha_{12}$. The blot was reprobed with antibodies to GAPDH to monitor equal loading of proteins. (C) Effect of $G\alpha_{12}$QL-CM on PDGFRα phosphorylation. $G\alpha_{12}$QL-NIH 3T3 cells and pcDNA3-NIH 3T3 cells (4×10^5 cells/100-mm plate) were grown for 16 h, followed by serum starvation for 24 h. The medium from pcDNA3-NIH 3T3 cells was replaced with CM from $G\alpha_{12}$QL-NIH 3T3 cells and incubated for 10 min. Lysates from serum-starved pcDNA3-NIH 3T3 cells (lane 1), pcDNA3-NIH 3T3 cells treated with CM (lane 2), and pc$G\alpha_{12}$QL-NIH 3T3 cells treated with CM in which PDGF-A was immunodepleted (lane 3) were subjected to immunoprecipitation with antibodies to PDGFRα antibodies, followed by immunoblot analysis with antibodies to P-Tyr (top). The same blot was reprobed with antibodies to PDGFRα after stripping (bottom). IB, immunoblot; Ab, antibody.

Downloaded from http://mcb.asm.org/ on September 23, 2019 by guest

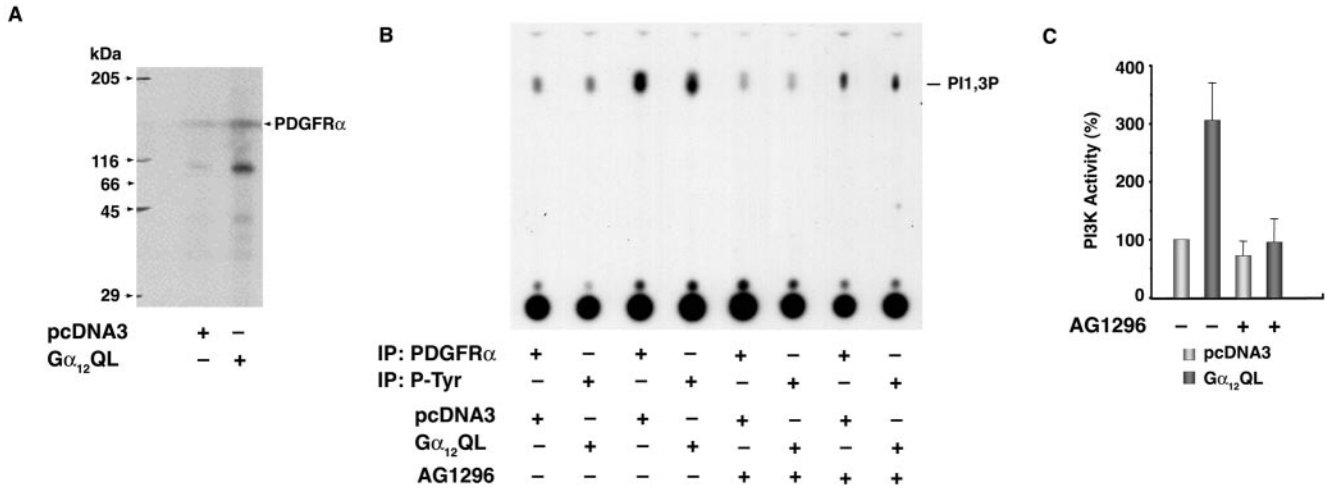

FIG. 5. $G\alpha_{12}$QL-stimulated PDGFRα activates PI3K. (A) $G\alpha_{12}$QL stimulates the autophosphorylation of PDGFRα. NIH 3T3 cells stably expressing $G\alpha_{12}$QL or pcDNA3 vector were serum starved for 24 h and PDGFRα was immunoprecipitated from the lysates using antibodies to PDGFRα. An immunocomplex kinase assay was carried out as described in Materials and Methods. The phosphorylated proteins were separated by SDS-PAGE and visualized by autoradiography. The band corresponding to the molecular size of PDGFRα is labeled. (B) $G\alpha_{12}$QL stimulates PDGFRα-associated PI3K. $G\alpha_{12}$QL-NIH 3T3 and pcDNA3-NIH 3T3 cells were serum starved for 24 h. They were pretreated with AG1296 (10 μM) or the vehicle dimethyl sulfoxide for 18 h, and the lysates were prepared using PI3K lysis buffer (see Materials and Methods). PDGFRα in the lysates (200 μg) was precipitated using antibodies to PDGFRα and assayed for PI3K activity using 5 μg of phosphotidylinositol as a substrate. The phosphorylated inositols were resolved by ascending TLC on a silica gel plate developed by $CHCl3 \cdot CH3OH \cdot NH_4OH$ (9: 7: 2) and visualized by autoradiography. A representative autoradiographic analysis of a chromatogram is presented. (C) $G\alpha_{12}$QL-stimulated PI3K activity is inhibited by PDGFR inhibitor. PI3K activity in the presence and absence of AG1296 (10 μM) in $G\alpha_{12}$QL-NIH 3T3 and pcDNA3-NIH 3T3 cells was analyzed. The phosphorylated inositols were resolved by ascending TLC on a silica gel plate developed by $CHCl3 \cdot CH3OH \cdot NH_4OH$ (9:7:2) and visualized by autoradiography. The PI3-P spots were quantified using Kodak 1D Image analysis software. The amount of phosphatidylinositol 3-phosphate formed, an index of PI3K activity, is presented as the percent increase over the vector control cells (mean ± SEM; $n = 3$). IP, immunoprecipitate.

strongly suggest that $G\alpha_{12}$QL stimulates an autocrine signaling loop leading to the activation of PDGFRα via PDGF-A.

$G\alpha_{12}$-transactivated PDGFR stimulates the PI3K-AKT signaling pathway. In vitro autophosphorylating activity of PDGFR has been widely used as an index of its functional activation (46). To further demonstrate that the expressed receptors are functional, an in vitro immunocomplex auto-kinase assay was carried out using PDGFRα immunoprecipitated with antibodies to PDGFRα. Results from this analysis of the autophosphorylation of PDGFRα indicated that there was an increase in the auto-kinase activity due to the transphosphorylation by PDGFRα in $G\alpha_{12}$QL-NIH 3T3 cells (Fig. 5A). PDGFRα stimulates a multitude of downstream effector molecules including PI3K, phospholipase C-gamma, Grb2/Sos1, Stats, Src, and SHP-2 (18). These molecules often integrate with each other in costimulating pathways involved in cell proliferation and cell survival while attenuating apoptotic pathways. While it is possible that the transactivation of PDGFRα by $G\alpha_{12}$QL generates such multiple signaling inputs, the PDGFRα-mediated activation of a PI3K-AKT signaling pathway is of great interest. It has been known that the pathways regulated by PI3K and AKT stimulate the expression of molecules involved in cell proliferation while downregulating the ones involved in apoptosis (29). Therefore, it can be speculated that $G\alpha_{12}$QL promotes serum-independent neoplastic cell growth by stimulating PI3K and AKT activities through PDGFRα. To examine such a role for PI3K in the $G\alpha_{12}$QL-PDGFR signaling alliance, we first determined whether PI3K is associated with PDGFRα and is activated in $G\alpha_{12}$QL-expressing cells. PDGFRα was immunoprecipitated from $G\alpha_{12}$QL-NIH 3T3 or the vector control cells using antibodies to PDGFRα and subjected to a PI3K assay using phosphotidylinositol as the substrate. The phosphorylated phospho-inositols were then separated using TLC. An increase in PDGFRα-associated PI3K activity, which can be inhibited by AG1296, a PDGFR-specific inhibitor, was seen in $G\alpha_{12}$QL cells (Fig. 5B and C). Quantification of the results showed that $G\alpha_{12}$QL stimulates PI3K activity by threefold (Fig. 5C). More interestingly, this increase could be inhibited strongly (70%) by treating the cells with the PDGFR inhibitor AG1296 (Fig. 5C).

To determine if $G\alpha_{12}$QL-stimulated PI3K activity results in the activation of AKT, the presence of activated AKT in $G\alpha_{12}$QL-NIH 3T3 cells was analyzed. Immunoblot analyses with antibodies to activated phospho-AKT indicated the activation of AKT in these cells (Fig. 6A). Inhibition of AKT activity by treating the cells with the PDGFR inhibitor AG1296 or the PI3K inhibitor Wortmannin clearly suggests that the activation of AKT in $G\alpha_{12}$QL-NIH 3T3 cells is PDGFRα and PI3K dependent (Fig. 6A and B). While our results presented here provide evidence that the increased levels of PDGFRα seen in the $G\alpha_{12}$QL cells contribute to the activation of associated PI3K and the downstream AKT activation, it is possible that $G\alpha_{12}$QL may also interact with additional signaling pathways in activating PI3K and AKT independent of PDGFRα. The observation that the inhibition of $G\alpha_{12}$QL-mediated activation of AKT by PDGFR inhibitor was not as complete as in the case of the PI3K inhibitor Wortmannin (70% versus 100%) (Fig. 6B) points to such an interesting possibility.

Downloaded from http://mcb.asm.org/ on September 23, 2019 by guest

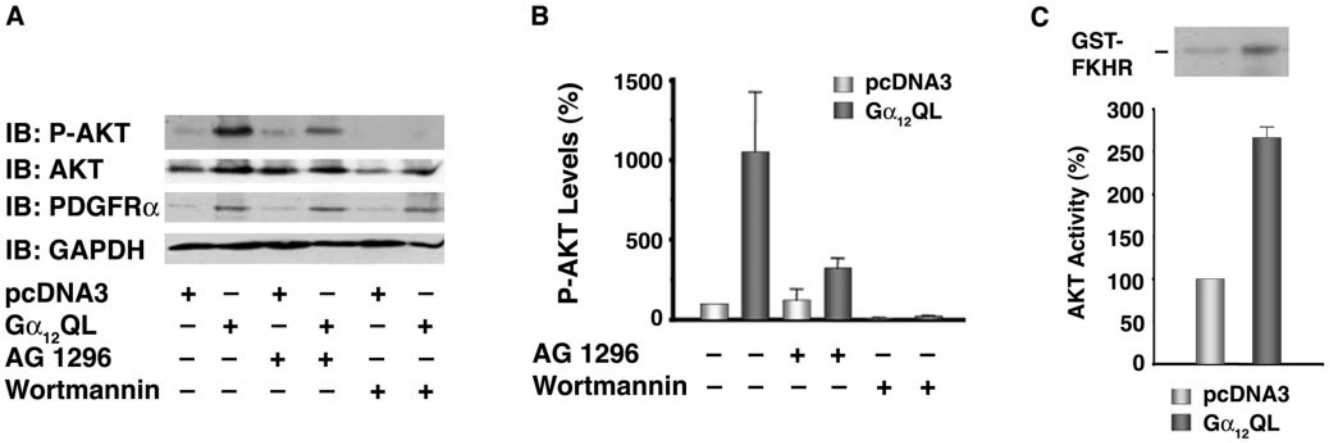

FIG. 6. $G\alpha_{12}QL$ stimulates AKT via PDGFRα and PI3K. (A) $G\alpha_{12}QL$ stimulates the phosphorylation of AKT. $G\alpha_{12}QL$-NIH 3T3 and pcDNA3-NIH 3T3 cells were serum starved for 24 h. Prior to lysis the cells were treated with 10 μM AG1296 (for 18 h) or 500 μM Wortmannin (2 h) or the vehicle dimethyl sulfoxide (0.1%). Immunoblot analysis was carried out with antibodies to phospho-AKT, followed by stripping and reprobing with antibodies to AKT. The blot was further analyzed for the expression of PDGFRα and GAPDH using antibodies to PDGFRα and GAPDH, respectively. Results from a typical experiment are presented. (B) $G\alpha_{12}QL$-mediated stimulation of AKT is inhibited by PDGFRα and PI3K inhibitors. $G\alpha_{12}QL$-NIH 3T3 and pcDNA3-NIH 3T3 cells were serum starved for 24 h. Prior to lysis the cells were treated with 10 μM AG1296 (for 18 h) or 500 nM Wortmannin (2 h) or the vehicle dimethyl sulfoxide (0.1%). Immunoblot analysis was carried out with antibodies to phospho-AKT. The expression levels of phospho-AKT bands were quantified using Kodak 1D image analysis software. AKT activity is presented as the percent increase over the vector control group (mean ± SEM; $n = 3$). (C) $G\alpha_{12}QL$ stimulates the kinase activity of AKT. AKT was immunoprecipitated with antibodies to AKT from the lysates of serum-starved $G\alpha_{12}QL$- and pcDNA3-NIH 3T3 cells. An immunocomplex kinase assay was carried out using purified recombinant FKHR as a substrate. The phosphorylated FKHR were separated by SDS-PAGE and visualized by autoradiography (top). Phosphorylated FKHR bands were excised and counted in a scintillation counter. AKT activity is expressed as the percent increase over the pcDNA3-NIH 3T3 control group (bottom). IB, immunoblot.

One of the major mechanisms through which AKT transduces the signals for cell survival and proliferation with a simultaneous decrease in antiproliferative and apoptotic signals is through phosphorylation of the forkhead family of transcription factors (FKHR) (4, 29). Unphosphorylated FKHR translocate to the nucleus and promote the expression of antiproliferative genes such as $p27^{Kip1}$ (28). However, upon phosphorylation by AKT, they are sequestered in the cytosol and prevented from transcribing both the apoptotic and antiproliferative genes (4, 28, 29). To determine whether the phosphorylated AKT seen in $G\alpha_{12}QL$-NIH 3T3 cells can mediate such inhibitory phosphorylation of FKHR, an in vitro kinase assay was performed using recombinant GST-FKHR as a substrate. Results from these experiments indicated that the kinase activity of AKT in phosphorylating FKHR is increased in $G\alpha_{12}QL$-expressing cells by more than twofold (Fig. 6C). Thus, our results clearly indicate that AKT, activated by $G\alpha_{12}QL$ via the PDGFR-PI3K signaling pathway, can phosphorylate FKHR.

To further demonstrate that inhibitory phosphorylation of forkhead transcription factors occurs in $G\alpha_{12}QL$-NIH 3T3 transformants in vivo, an immunoblot analysis was carried out using antibodies directed against *for*k*h*ead transcription factor in *r*habdomyosarcoma-*l*ike factor 1 (FKHRL1) or FOXO3a, a member of the forkhead family of transcription factors. Lysates from $G\alpha_{12}QL$-NIH 3T3 cells along with vector control cells were examined for the phosphorylation of FKHRL1 by immunoblot analysis using antibodies to phospho-FKHRL1. The immunoblot analysis clearly indicated that the phosphorylation of FKHRL1 is increased in $G\alpha_{12}QL$-NIH 3T3 cells (Fig. 7A). To define the role of PI3K and PDGFRα in $G\alpha_{12}QL$-stimulated phosphorylation of FKHRL1, we examined the phosphorylation levels of FKHRL1 in $G\alpha_{12}QL$ cells with the PI3K inhibitor Wortmannin or the PDGFR inhibitor AG1296. As expected, treatment of cells with Wortmannin completely inhibited the $G\alpha_{12}QL$-stimulated phosphorylation of FKHRL1 (Fig. 7B). More significantly, treatment of cells with AG1296 drastically decreased the levels of phosphorylation in FKHRL1 (Fig. 7C), similar to its effect on AKT phosphorylation (Fig. 6A and B). Taken together, these results suggest a linear pathway involving PDGFRα, PI3K, and AKT in $G\alpha_{12}QL$-mediated phosphorylation of FKHRL1.

Increased phosphorylation of FKHRL1 by AKT in $G\alpha_{12}QL$-NIH 3T3 cells would suggest that the FKHR are being prevented from binding to their target response elements to transactivate the expression of antiproliferative genes such as cyclin-dependent kinase inhibitors, thereby promoting the accelerated proliferation of these cells (4, 28, 29). In order to demonstrate that such binding of FKHRL1 to its response element is indeed decreased in $G\alpha_{12}QL$-NIH 3T3 cells, we carried out an electrophoretic mobility shift assay. Nuclear extracts were prepared from both $G\alpha_{12}QL$-NIH 3T3 and vector control pcDNA3 cells and an in vitro DNA-binding assay was carried out by gel shift analysis using an oligonucleotide probe containing three forkhead responsive elements in tandem. The nucleoprotein complex, as indicated by the specific gel shift band, is greatly reduced in $G\alpha_{12}QL$-NIH 3T3 cells (Fig. 7D, lane 3 versus lane 4). FKHRL1 antibody was able to supershift this complex, thus demonstrating the specificity of FKHRL1 binding to its response element (Fig. 7D, lanes 5 and 6). Furthermore, the DNA-protein complex was efficiently dissociated in the presence of the cold competitor (Fig. 7D, lanes 1 and 2). These results clearly indicate that the DNA-binding activity of

Downloaded from http://mcb.asm.org/ on September 23, 2019 by guest

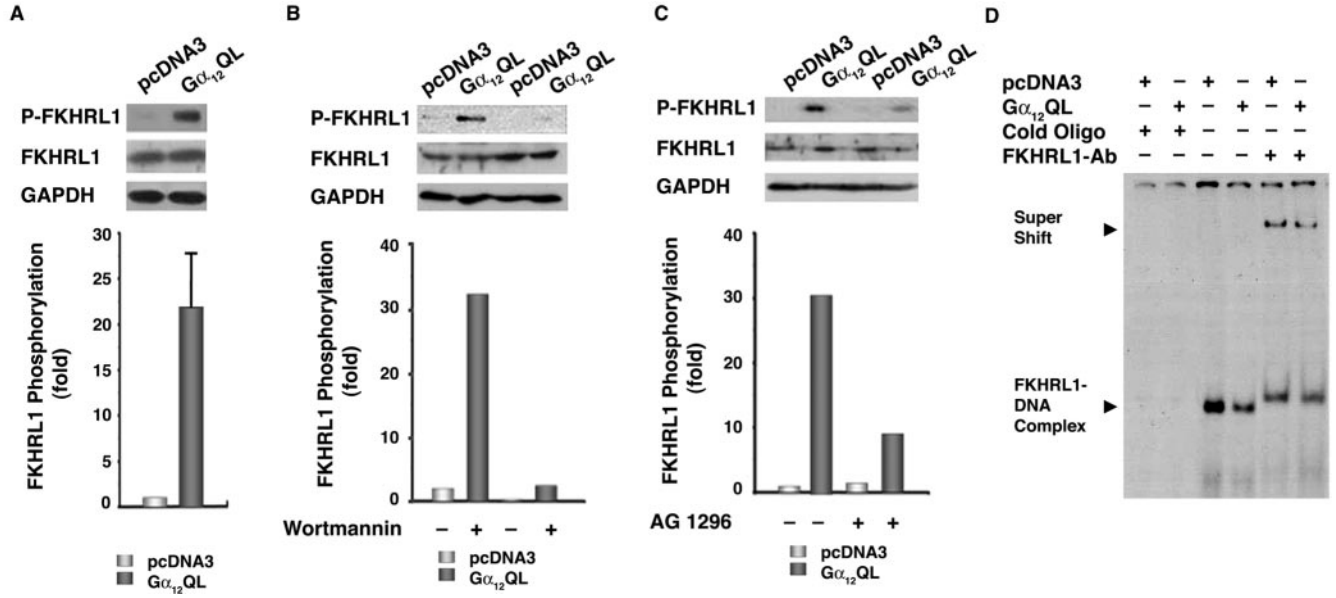

FIG. 7. $G\alpha_{12}$QL inhibits FKHRL1 activity. (A) $G\alpha_{12}$QL stimulates the inhibitory phosphorylation of forkhead transcription factor FKHRL1. Lysates from serum-starved $G\alpha_{12}$QL- and pcDNA3-NIH 3T3 cells were subjected to immunoblot analysis with antibodies to phospho-FKHRL1. The blot was sequentially stripped and reprobed with antibodies to FKHRL1 and GAPDH. The levels of FKHRL1 phosphorylation were quantified by Kodak 1D image analysis software. FKHRL1 phosphorylation is presented as the increase over the pcDNA3-NIH 3T3 cell control group. (B) Phosphorylation of FKHRL1 by $G\alpha_{12}$QL is dependent on PI3K. $G\alpha_{12}$QL-NIH 3T3 and pcDNA3-NIH 3T3 cells were serum starved (24 h). Prior to lysis the cells were treated with Wortmannin (2 h) along with the vehicle control (0.1% dimethyl sulfoxide). Immunoblot analysis was carried out with the cell lysates using antibodies to phospho-FKHRL1, followed by sequential stripping and reprobing with antibodies to FKHRL1 and GAPDH, respectively (top). The levels of phosphorylated FKHRL1 bands were quantified by Kodak 1D image analysis software. The results are presented as the increase in the levels of phosphorylated FKHRL1 over the untreated pcDNA3-NIH 3T3 vector control cells (bottom). (C) Phosphorylation of FKHRL1 by $G\alpha_{12}$QL is PDGFRα dependent. $G\alpha_{12}$QL-NIH 3T3 and pcDNA3-NIH 3T3 cells were serum starved (24 h). Prior to lysis the cells were treated with 10 μM AG1296 (18 h) along with the vehicle control (0.1% dimethyl sulfoxide). Immunoblot analysis was carried out with the cell lysates using antibodies to phospho-FKHRL1 followed by sequential stripping and reprobing with antibodies to FKHRL1 and GAPDH, respectively (top) The levels of phosphorylated FKHRL1 bands were quantified by Kodak 1D image analysis software. The results are presented as the increase in the levels of phosphorylated FKHRL1 over the untreated pcDNA3-NIH 3T3 vector control cells (bottom). (D) FKHRL1 binding to its response elements is attenuated in cells expressing $G\alpha_{12}$QL. Electromobility shift assays were performed with nuclear extracts from 24-h serum-starved $G\alpha_{12}$QL- and pcDNA3-NIH 3T3 cells and radiolabeled oligonucleotide probes containing FKHRL1 binding sites as described in Materials and Methods. The nuclear extracts prepared from pcDNA3- and $G\alpha_{12}$QL-NIH 3T3 cells were incubated with radiolabeled oligonucleotide containing FKHRL1 response elements alone (lanes 3 and 4), with competing cold oligonucleotide (lanes 1 and 2) or with antibodies to FKRHL1 (lanes 5 and 6).

FKHRL1 is inhibited in $G\alpha_{12}$QL-NIH 3T3 cells. Since decreased binding of FKHRL1 to its promoter has been strongly associated with cell proliferation (4, 28, 29), these results point to a hitherto unknown mechanism through which $G\alpha_{12}$ can promote cell growth.

Dominant negative mutant of PDGFRα inhibits $G\alpha_{12}$QL-mediated focus formation. Our results presented here thus far have shown the following: (i) that the activated mutant of $G\alpha_{12}$ increases the expression as well as the activation of PDGFRα (Fig. 1 to 4), (ii) that activated PDGFRα in turn activates the PI3K/AKT pathway (Fig. 5 and 6), and (iii) that the activated PI3K-AKT pathway stimulates the inhibitory phosphorylation of forkhead transcription factor FKHRL1, a gene that has been previously shown to be involved in the transcription of antiproliferation genes (Fig. 7). Based on these findings, it can be speculated that the increased expression and activation of PDGFRα may play a role in $G\alpha_{12}$-mediated oncogenic pathways. $G\alpha_{12}$-transformed fibroblasts, in addition to exhibiting increased proliferation, show other transformed phenotypes such as anchorage-independent cell growth and loss of contact inhibition (5, 35). The focus formation assay has been widely used to define the signaling nodes involved in oncogenic pathways (8, 10). Therefore, we further explored whether PDGFRα plays a role in $G\alpha_{12}$-mediated focus formation. It has been demonstrated that the deletion of the C terminus of PDGFRα results in a dominant negative phenotype (22). Using this dominant negative mutant of PDGFRα (DN-PDGFRα), we investigated whether functional signaling by PDGFRα is required for $G\alpha_{12}$QL-mediated focus formation of NIH 3T3 cells. NIH 3T3 cells were transfected with vector containing $G\alpha_{12}$QL or the empty vector pcDNA3, along with pcDNA3 carrying the truncated mutant of PDGFRα. The numbers of foci were scored 10 to 14 days posttransfection. The results show that while $G\alpha_{12}$QL induces focus formation in NIH 3T3 cells (Fig. 8A and B), the number of foci induced by $G\alpha_{12}$QL is reduced in the presence of DN-PDGFRα (Fig. 8C). Quantification of results from repeat experiments indicated that the number of foci induced by $G\alpha_{12}$QL was reduced by 40% in the presence of DN-PDGFRα (Fig. 8D). These results suggest that PDGFRα is involved in $G\alpha_{12}$QL-mediated loss of contact-inhibited growth of NIH 3T3 cells.

Downloaded from http://mcb.asm.org/ on September 23, 2019 by guest

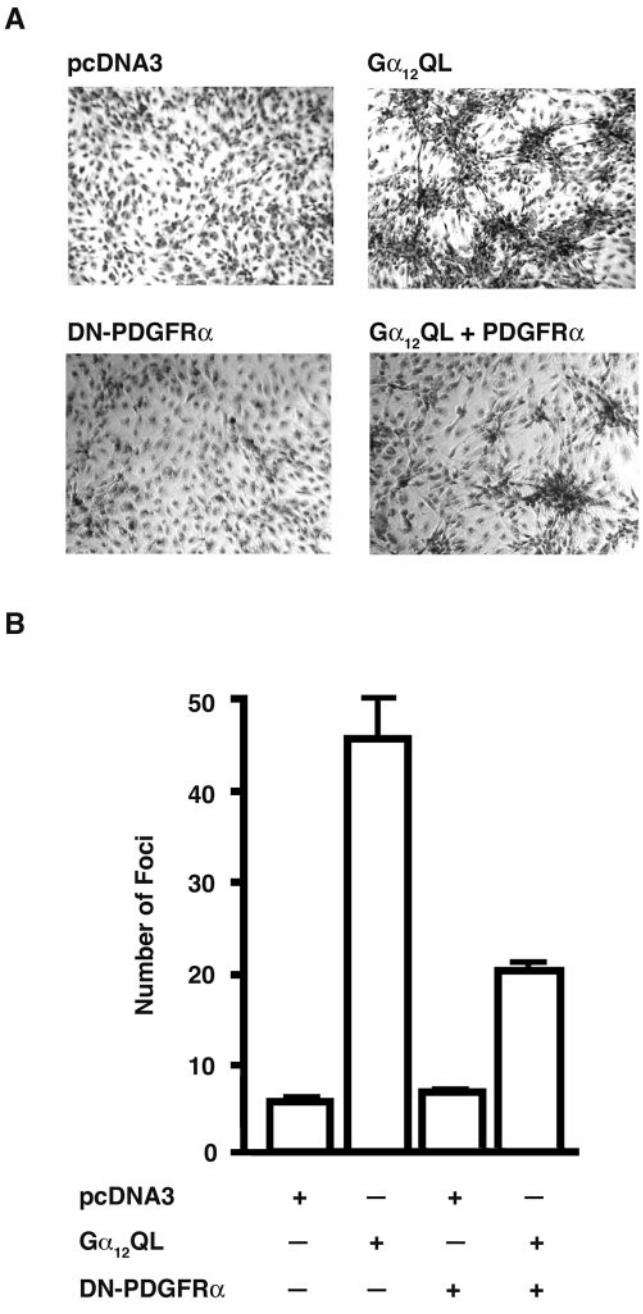

FIG. 8. Dominant negative mutant of PDGFRα inhibits $G\alpha_{12}$QL-mediated focus formation. (A) Parental NIH 3T3 cells were transfected with the activated mutant of $G\alpha_{12}$ ($G\alpha_{12}$QL), empty vector (pcDNA3), DN-PDGFRα, or $G\alpha_{12}$QL plus DN-PDGFRα ($G\alpha_{12}$QL+DN-PDGFRα) using the calcium phosphate transfection method as described in Materials and Methods. The representative foci formed at 14 days were photographed at ×4 magnification. (B) The number of foci formed from two independent experiments were scored and plotted (mean ± standard deviation).

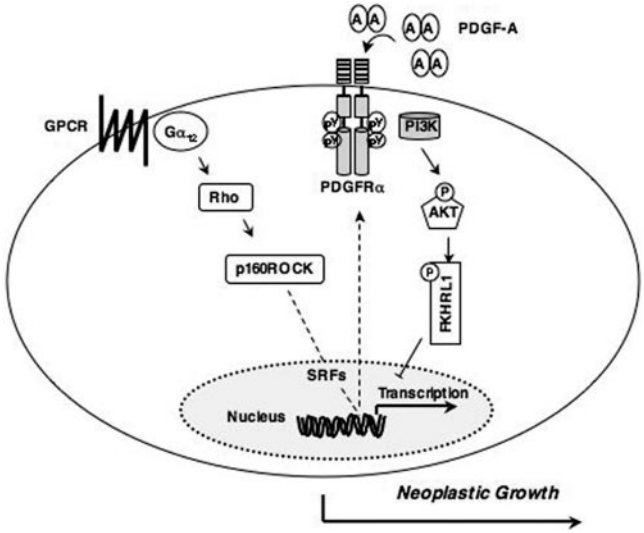

FIG. 9. Schematic representation of $G\alpha_{12}$-mediated activation of PDGFRα signaling pathway. Activated $G\alpha_{12}$ stimulates the expression of PDGFRα via a Rho-dependent signaling pathway. The increased expression of PDGF-A in these cells stimulates PDGFRα, thus forming an autocrine signaling loop. The $G\alpha_{12}$-stimulated PDGFRα engages the downstream PI3K-AKT signaling pathway to inhibit FKHRL1-mediated transcription of apoptotic and antiproliferative genes to promote neoplastic cell growth.

DISCUSSION

To date, several independent studies have confirmed that activated $G\alpha_{12}$, when transfected, confers transformed phenotypes to fibroblast cell lines (5, 11, 35). In addition, $G\alpha_{12}$ has been shown to stimulate proliferation in many different cell lines. In addition, similar to other potent oncogenes (16), the activated mutant of $G\alpha_{12}$ can promote serum-independent cell growth (Fig. 1). These studies have identified that the mitogenic signaling by $G\alpha_{12}$ involves inputs from multiple signaling pathways emanating from the Ras as well as Rho family of GTPases, JNK, COX2, and β-catenin (5, 11, 31, 35). While these studies have suggested that $G\alpha_{12}$ is critically involved in cell growth regulation, the molecular mechanisms involved in this process of transformation or proliferation remain obscure. In this context, our finding that the activation of $G\alpha_{12}$ stimulates the expression as well as the activation of the potent mitogenic receptor tyrosine kinase PDGFRα is quite significant. These findings gain further significance in light of the observation that thrombin and LPA, the major growth-promoting GPCR ligands in circulating serum that can stimulate $G\alpha_{12}$, increase the expression and activation of PDGFRα (Fig. 1D and 3E). Together with our observations that the inhibition of PDGFR, even with the suboptimal dose of AG1296 (5 μM), can attenuate the proliferation in $G\alpha_{12}$QL-NIH 3T3 cells (25) and that the coexpression of a dominant negative mutant of PDGFRα attenuates $G\alpha_{12}$QL-mediated focus formation of NIH 3T3 cells by 40% (Fig. 8), our results presented here identify PDGFRα as a major signaling channel through which $G\alpha_{12}$ transmits its mitogenic signals in its multiplex signaling network (Fig. 9).

The study presented here identifies several novel aspects in $G\alpha_{12}$ signaling. These novel findings include our observations that the regulation of PDGFRα is specific to $G\alpha_{12}$ and not to the closely related transforming oncogene $G\alpha_{13}$ (Fig. 1A to C); that LPA and thrombin, which stimulate $G\alpha_{12}$ (via their cognate receptors), enhance the expression/activation of PDGFRα (Fig. 1D and 3E); that $G\alpha_{12}$QL-mediated enhanced expression of

Downloaded from http://mcb.asm.org/ on September 23, 2019 by guest

PDGFRα involves the small GTPase Rho (Fig. 2A and B); that the constitutively activated mutant of Rho can stimulate the expression of PDGFRα (Fig. 2B); that $G\alpha_{12}$ increases the expression of PDGF-A message as well as protein (Fig. 4A and B); that CM from $G\alpha_{12}$QL stimulates the phosphorylation of PDGFRα and the stimulation of PDGFRα phosphorylation by $G\alpha_{12}$QL-CM is lost when PDGF-A was immuno-depleted from such medium (Fig. 4C); that $G\alpha_{12}$ stimulates the PI3K-AKT-FKHR signaling conduit via PDGFRα (Fig. 5 to 7); and that $G\alpha_{12}$QL-mediated focus formation of NIH 3T3 cells is inhibited by the coexpression of the dominant negative mutant of PDGFRα (19). With these findings, our studies provide for the first time the mechanism through which $G\alpha_{12}$ coordinates a signaling network involving PDGFRα to promote neoplastic cell growth (Fig. 9).

The finding that $G\alpha_{12}$ stimulates the expression as well as transactivation of PDGFRα suggests that $G\alpha_{12}$ stimulates PDGFRα signaling at two distinct loci. The expression levels of PDGFRα appear to be stimulated through a RhoA-p160ROCK-dependent signaling pathway (Fig. 3), whereas the transactivation of PDGFRα appears to involve an autocrine loop, as suggested by the CM experiment (Fig. 4). Preliminary studies show that Rho is not involved in the expression of PDGF ligands (data not shown). The data showing the involvement of Rho in $G\alpha_{12}$-mediated expression of PDGFRα are consistent with previous findings that $G\alpha_{12}$ activates serum response factors through a RhoA-p160ROCK-dependent signaling pathway (14). However, it should be noted here that the previous studies demonstrating the role of Rho in mediating $G\alpha_{12}$-stimulated gene expression are through the use of reporter assays using serum response elements containing reporter constructs (14). While these studies certainly pointed out the importance of Rho signaling in a $G\alpha_{12}$-mediated signaling pathway, our finding here showing that $G\alpha_{12}$QL stimulates the expression of PDGFRα via Rho is, rather, a first report showing a direct role of Rho in stimulating the expression of a critical receptor kinase in the $G\alpha_{12}$QL signaling pathway.

The observation that $G\alpha_{12}$-activated PDGFRα stimulates the PI3K-AKT pathway leading to the phosphorylation and inactivation of forkhead transcription factors is quite significant in that it can provide a central mechanism by which $G\alpha_{12}$ can attenuate apoptotic signals while increasing signals for cell survival and growth. Thus, our studies presented here suggest that such $G\alpha_{12}$QL-PDGFRα-PI3K-AKT-mediated inhibition of FKHR (Fig. 5 to 7) would synergize with other $G\alpha_{12}$-signaling inputs to promote neoplastic transformation of NIH 3T3 cells. Although the ability of PDGFRα to stimulate PI3K and the effect of PI3K-AKT signaling on FKHRL1 are rather anticipated, our findings gain significance in light of the observation that $G\alpha_{12}$ recruits the PDGFRα-PI3K-AKT-FKHRL1 signaling conduit to promote neoplastic cell growth. That the inhibition of the upstream signaling node of this pathway, namely, PDGFRα, attenuates the $G\alpha_{12}$QL-mediated oncogenic phenotype (Fig. 8) is highly significant and establishes the critical role of this signaling axis in $G\alpha_{12}$QL-mediated neoplastic cell growth. Taken together, these observations that the inhibition of PDGFR using the PDGFR inhibitor AG1296 attenuates $G\alpha_{12}$-mediated proliferation (25) and that the coexpression of the dominant negative mutant of PDGFRα inhibits $G\alpha_{12}$-mediated focus formation in NIH 3T3 cells (Fig. 8) identify PDGFRα as one of the major signaling conduits through which $G\alpha_{12}$ transmits its proliferative signals.

These findings gain more significance in light of the recent observations that link G protein-coupled LPA receptors and PDGFRα in the genesis of ovarian cancers. Levels of LPA in serum and ascites are elevated in ovarian cancer patients (13). Interestingly, LPA, at concentrations present in ascitic fluid, has been shown to stimulate the growth of malignant ovarian tumors (21). A recent study has also shown that 39% of ovarian tumors overexpress PDGFRα and, hence, PDGFRα has been identified as an ovarian cancer-specific gene (30). Several studies have demonstrated cross talk between G protein-coupled receptors and receptor tyrosine kinases in tumorigenesis. Considering the findings that LPA stimulates its cognate receptors coupled to G12, it is possible that such cross talk involving $G\alpha_{12}$ and PDGFRα exists in the ovarian cancer cells. Thus, it can be hypothesized that in ovarian carcinoma, LPA activates $G\alpha_{12}$, which, in turn, regulates PDGFRα and its downstream signaling pathways. The observation by Gutkind et al. that $G\alpha_{12}$ is overexpressed in ovarian cancers (15) and our observation that LPA stimulates the expression of PDGFRα in C272 ovarian carcinoma cells (R. N. Kumar and D. N. Dhanasekaran, unpublished observation) give credence to such a hypothesis. As ovarian cancers form a group of neoplasms with very poor prognosis, identifying new biomarkers and dissecting the signaling inputs and multiple pathways involved in contributing to their malignancy are of prime importance. Now that our results have identified the possible coupling mechanism between activated $G\alpha_{12}$ and PDGFRα levels, we are pursuing studies to define the role of the signaling network involving LPA, LPA-stimulated $G\alpha_{12}$, and $G\alpha_{12}$-stimulated overexpression/transactivation of PDGFRα on the genesis and progression of ovarian cancer cell growth.

ACKNOWLEDGMENTS

We are grateful to Andrius Kazlauskas for the dominant negative mutant construct of PDGFRα and Aviv Hassid for the adenoviral vectors encoding RhoA-G14V as well as RhoA-T19N. We are also grateful to Gary Bokoch for the pGEX 2T-GST-RBD construct. The critical reading of the manuscript by Kimia Kashef and Zachariah Goldsmith is gratefully appreciated.

This work was supported by grants from the National Institutes of Health (GM49897).

REFERENCES

1. **Aragay, A. M., L. R. Collins, G. R. Post, A. J. Watson, J. R. Feramisco, J. H. Brown, and M. I Simon.** 1995. G12 requirement for thrombin-stimulated gene expression and DNA synthesis in 1321N1 astrocytoma cells. J. Biol. Chem. **270:**20073–20077.
2. **Baudhuin, L. M., Y. Jiang, A. Zaslawsky, I. Ishii, J. Chun, and Y. Xu.** 2004. S1P3-mediated Akt activation and cross-talk with platelet-derived growth factor receptor (PDGFR). FASEB J. **18:**341–343.
3. **Benard, V., and G. M. Bokoch.** 2002. Assay of Cdc42, Rac, and Rho GTPase activation by affinity methods. Methods Enzymol. **345:**349–359.
4. **Birkenkamp, K. U., and P. J. Coffer.** 2003. Regulation of cell survival and proliferation by the FOXO (Forkhead box, class O) subfamily of Forkhead transcription factors. Biochem. Soc. Trans. **31:**292–297.
5. **Chan, A. M., T. P. Fleming, E. S. McGovern, M. Chedid, T. Miki, and S. A. Aaronson.** 1993. Expression cDNA cloning of a transforming gene encoding the wild-type $G\alpha_{12}$ gene product. Mol. Cell. Biol. **2:**762–768.
6. **Chang, Y., B. Ceacareanu, M. Dixi, N. Sreejayan, and A. Hassid.** 2002. Nitric oxide-induced motility in aortic smooth muscle cells. Role of protein tyrosine phosphatase SHP-2 and GTP-binding protein Rho. Circ. Res. **91:**390–397.
7. **Collins, L. R., W. A. Ricketts, J. M. Olefsky, and J. H. Brown.** 1997. The G12 coupled thrombin receptor stimulates mitogenesis through the Shc SH2 domain. Oncogene **15:**595–600.

Downloaded from http://mcb.asm.org/ on September 23, 2019 by guest

8. **Cox, A. D., and C. J. Der.** 1994. Biological assays for cellular transformation. Methods Enzymol. **238:**277–294.
9. **Dai, C., J. C. Celestino, Y. Okada, D. N. Louis, G. N. Fuller, and E. C. Holland.** 2001. PDGF autocrine stimulation dedifferentiates cultured astrocytes and induces oligodendrogliomas and oligoastrocytomas from neural progenitors and astrocytes in vivo. Genes Dev. **15:**1913–1925.
10. **Dermott, J. M., and N. Dhanasekaran.** 2002. Determining cellular role of $G\alpha_{12}$. Methods Enzymol. **344:**298–309.
11. **Dhanasekaran, N., and J. M. Dermott.** 1996. Signaling by the G12 class of G proteins. Cell Signal. **8:**235–245.
12. **Ding, H., A. Nagy, D. H. Guttman, and A. Guha.** 2000. A review of astrocytoma models. Neurosurg. Focus **8:**1–8.
13. **Fang, X., D. Gaudette, T. Furui, M. Mao, V. Estrella, A. Eder, T. Pustilnik, T. Sasagawa, R. Lapushin, S. Yu, R. B. Jaffe, J. R. Wiener, J. R. Erickson, and G. B Mills.** 2000. Lysophospholipid growth factors in the initiation, progression, metastases, and management of ovarian cancer. Ann. N. Y. Acad. Sci. **905:**188–208.
14. **Fromm, C., O. A. Coso, S. Montaner, N. Xu, and J. S. Gutkind.** 1997. The small GTP-binding protein Rho links G protein-coupled receptors and $G\alpha_{12}$ to the serum response element and to cellular transformation. Proc. Natl. Acad. Sci. USA **94:**10098–10103.
15. **Gutkind, J. S., O. A. Coso, and N. Xu.** 1998. $G\alpha_{12}$- and $G\alpha_{13}$-subunits of heterotrimeric G proteins: a novel family of oncogenes, p. 101–117. *In* S. Spiegel (ed.), G proteins, receptors, and diseases ed. Humana Press, Totowa, N.J.
16. **Hanahan, D., and R. A. Weinberg.** 2000. The hallmarks of cancer. Cell **100:**57–70.
17. **Heinrich, M. C., C. L. Corless, A. Duensing, L. McGreevey, C. J. Chen, N. Joseph, S. Singer, D. J. Griffith, A. Haley, A. Town, G. D. Demetri, C. D. Fletcher, and J. A. Fletcher.** 2003. PDGFRA activating mutations in gastrointestinal stromal tumors. Science **299:**708–710.
18. **Heldin, C. H., A. Ostman, and L. Ronnstrand.** 1998. Signal transduction via platelet-derived growth factor receptors. Biochim. Biophys. Acta **1378:**F79–F113.
19. **Henriksen, R., K. Funa, E. Wilander, T. Backstrom, M. Ridderheim, and K. Oberg.** 1993. Expression and prognostic significance of platelet-derived growth factor and its receptors in epithelial ovarian neoplasms. Cancer Res. **53:**4550–4554.
20. **Herrlich, A., H. Daub, A. Knebel, P. Herrlich, A. Ullrich, G. Schultz, and T. Gudermann.** 1998. Ligand-independent activation of platelet-derived growth factor receptor is a necessary intermediate in lysophosphatidic, acid-stimulated mitogenic activity in L cells. Proc. Natl. Acad. Sci. USA **95:**8985–8990.
21. **Hu, Y. L., C. Albanese, R. G. Pestell, and R. B. Jaffe.** 2003. Dual mechanisms for lysophosphatidic acid stimulation of human ovarian carcinoma cells. J. Natl. Cancer Inst. **95:**733–740.
22. **Ikuno, Y., and A. Kazlauskas.** 2002. An in vivo gene therapy approach for experimental proliferative vitreoretinopathy using the truncated platelet-derived growth factor alpha receptor. Investig. Ophthalmol. Vis. Sci. **43:**2406–2411.
23. **Janssen, R. A., P. N. Kim, J. W. Mier, and D. K. Morrison.** 2003. Overexpression of kinase suppressor of Ras upregulates the high-molecular-weight tropomyosin isoforms in *ras*-transformed NIH 3T3 fibroblasts. Mol. Cell. Biol. **23:**1786–1797.
24. **Kawagishi, J., T. Kumabe, T. Yoshimoto, and T. Yamamoto.** 1995. Structure, organization, and transcription units of the human alpha-platelet-derived growth factor receptor gene, PDGFRA. Genomics **30:**224–232.
25. **Kumar, R. N., V. Radhika, V. Audigé, S. G. Rane, and N. Dhanasekaran.** 2004. Proliferation-specific genes activated by $G\alpha_{12}$. Cell Biochem. Biophys. **41:**63–73.
26. **Lin, T., L. Zeng, Y. Liu, K. DeFea, M. A. Schwartz, S. Chien, and J. Y.-J. Shyly.** 2003. Rho-ROCK-LIMK-Cofilin pathway regulates shear stress activation of sterol regulatory element binding proteins. Circ. Res. **92:**1296–1304.
27. **Lokker, N. A., C. M. Sullivan, S. J. Hollenbach, M. A. Israel, and N. A. Giese.** 2002. Platelet-derived growth factor (PDGF) autocrine signaling regulates survival and mitogenic pathways in glioblastoma cells: evidence that the novel PDGF-C and PDGF-D ligands may play a role in the development of brain tumors. Cancer Res. **62:**3729–3735.
28. **Martinez-Gac, L., M. Marques, Z. Garcia, M. R. Campanero, and A. C. Carrera.** 2004. Control of cyclin G2 mRNA expression by forkhead transcription factors: novel mechanism for cell cycle control by phosphoinositide 3-kinase and forkhead. Mol. Cell. Biol. **24:**2181–2189.
29. **Martinez-Gac, L., B. Alvarez, Z. Garcia, M. Marques, M. Arrizabalaga, and A. C. Carrera.** 2004. Phosphoinositide 3-kinase and forkhead, a switch for cell division. Biochem. Soc. Trans. **32:**360–361.
30. **Matei, D., D. D. Chang, and M. H. Jeng.** 2004. Imatinib mesylate (Gleevec) inhibits ovarian cancer cell growth through a mechanism dependent on platelet-derived growth factor receptor alpha and Akt inactivation. Clin. Cancer Res. **10:**681–690.
31. **Meigs, T. E., T. A. Fields, D. D. McKee, and P. J. Casey.** 2001. Interaction of $G\alpha12$ and $G\alpha13$ with the cytoplasmic domain of cadherin provides a mechanism for β-catenin release. Proc. Natl. Acad. Sci. USA **98:**519–524.
32. **Mondorf, U. F., H. Geiger, M. Herrero, S. Zeuzem, and A. Piiper.** 2000. Involvement of the platelet-derived growth factor receptor in angiotensin II-induced activation of extracellular regulated kinases 1 and 2 in human mesangial cells. FEBS Lett. **472:**129–132.
33. **Nebigil, C. G., J. M. Launay, P. Hickel, C. Tournois, and L. Maroteaux.** 2000. 5-hydroxytryptamine 2B receptor regulates cell-cycle progression: cross-talk with tyrosine kinase pathways. Proc. Natl. Acad. Sci. USA **97:**2591–2596.
34. **Pleiman, C. M., M. R. Clark, L. K. Gauen, S. Winitz, K. M. Coggeshall, G. L. Johnson, A. S. Shaw, and J. C. Cambier.** 1993. Mapping of sites on the Src family protein tyrosine kinases p55blk, p59fyn, and p56lyn, which interact with the effector molecules phospholipase C-gamma 2, microtubule-associated protein kinase, GTPase-activating protein, and phosphatidylinositol 3-kinase. Mol. Cell. Biol. **13:**5877–5887.
35. **Radhika, V., and N. Dhanasekaran.** 2001. Transforming G proteins. Oncogene **20:**1607–1614.
36. **Radhika, V., D. Onesime, J. H. Ha, and N. Dhanasekaran.** 2004. $G\alpha_{13}$ stimulates cell migration through cortactin-interacting protein Hax-1. J. Biol. Chem. **279:**49406–49413.
37. **Radhika, V., J. H. Ha, M. Jayaraman, S. T. Tsim, and N. Dhanasekaran.** 2005. Mitogenic signaling by lysophosphatidic acid (LPA) involves $G\alpha_{12}$. Oncogene **24:**4597–4603.
38. **Ren, X. D., and M. A. Schwartz.** 2000. Determination of GTP loading on Rho. Methods Enzymol. **325:**264–272.
39. **Saito, Y., and B. C. Berk.** 2001. Transactivation: a novel signaling pathway from angiotensin II to tyrosine kinase receptors. J. Mol. Cell. Cardiol. **33:**3–7.
40. **Seasholtz, T. M., J. Radeff-Huang, S. A. Sagi, R. Matteo, J. M. Weema, A. S. Cohen, J. R. Feramisco, and J. H. Brown.** 2004. Rho-mediated cytoskeletal rearrangement in response to LPA is functionally antagonized by Rac1 and PIP2. J. Neurochem. **91:**501–502.
41. **Tang, P., P. A. Steck, and W. K. Yung.** 1997. The autocrine loop of TGF-α/EGFR and brain tumors. J. Neurooncol. **35:**303–314.
42. **Uren, A., M. S. Merchant, C. J. Sun, M. I. Vitolo, Y. Sun, M. Tsokoa, P. B. Illei, M. Ladanyi, A. Passaniti, C. Mackall, and J. A. Toretsky.** 2003. Beta-platelet-derived growth factor receptor mediates motility and growth of Ewing's sarcoma cells. Oncogene **22:**2334–2342.
43. **Vara Prasad, M. V., S. K. Shore, and N. Dhanasekaran.** 1994. Activated mutant of $G\alpha_{13}$ induces Egr-1, c-fos, and transformation in NIH 3T3 cells. Oncogene **9:**2425–2429.
44. **Vara Prasad, M. V. V. S., J. M. Dermott, L. E. Heasley, G. L. Johnson, and N. Dhanasekaran.** 1995. Activation of Jun kinase/stress-activated protein kinase by GTPase-deficient mutants of $G\alpha_{12}$ and $G\alpha_{13}$. J. Biol. Chem. **270:**18655–18659.
45. **Xie, J., M. Aszterbaum, X. Zhang, J. M. Bonifas, C. Zachary, E. Epstein, and F. McCormick.** 2001. A role of PDGFRα in basal cell carcinoma proliferation. Proc. Natl. Acad. Sci. USA **98:**9255–9259.
46. **Yokote, K., B. Margolis, C. H. Heldin, and L. Claesson-Welsh.** 1996. Grb7 is a downstream signaling component of platelet-derived growth factor α- and β-receptors. J. Biol. Chem. **271:**30942–30949.

Downloaded from http://mcb.asm.org/ on September 23, 2019 by guest